Speed of Sound Measurements and a Fundamental Equation of State for Hydrogen Chloride

Monika Thol[1*], Frithjof H. Dubberke[2], Elmar Baumhögger[2], Roland Span[1], Jadran Vrabec[2]

[1]Lehrstuhl für Thermodynamik, Ruhr-Universität Bochum, Universitätsstraße 150, 44801 Bochum, Germany

[2]Lehrstuhl für Thermodynamik und Energietechnik, Universität Paderborn, Warburger Straße 100, 33098 Paderborn, Germany

Abstract

A fundamental equation of state in terms of the Helmholtz energy is presented for hydrogen chloride. Any thermodynamic property can be calculated by combinations of its derivatives with respect to the independent variables temperature and density. The present equation of state is applicable in the entire fluid region. Its accuracy is assessed by comparison with the available experimental literature data from the triple point temperature to 480 K and a maximum pressure of 40 MPa. A reasonable extrapolation behavior beyond these temperature and pressure limits is ensured to allow for an application to mixture models. For the development of the present equation of state, speed of sound measurements are carried out in the liquid and dense vapor phases by means of the pulse-echo technique. Because no speed of sound measurements for this fluid are reported in the literature, the present experimental dataset is crucial for the accurate modeling of caloric properties of hydrogen chloride.

[*]E-mail: M.Thol@thermo.ruhr-uni-bochum.de

1 Introduction

Hydrogen chloride (HCl, CAS No. 7647-01-0) is a toxic, colorless, and fetid gas, which is easily soluble in water. It has a strong penetrative odor and in contact with humid air it develops white fog due to its intense hygroscopicity.[1] Upon reaction with water, it yields hydrochloric acid, which aggressively corrodes a wide range of materials. The knowledge of thermophysical properties of hydrogen chloride is important for any application where even small amounts of this substance may be involved. Since hydrogen chloride is highly reactive, it does not occur in nature but is produced in the laboratory by a reaction of sodium chloride and sulfuric acid. In the chemical industry, it is mainly a byproduct of the chlorination of organic substances. Its main applications are the production of hydrochloric acid, the hydrochlorination of rubber, and the production of vinyl and alkyl chlorides.[2]

For the supply of thermodynamic properties, it is state of the art to develop fundamental equations of state in terms of the residual Helmholtz energy with the independent variables temperature and density. For the development of such correlations, information on the density in the homogeneous liquid phase, the vapor-liquid equilibrium, the critical point, and the isobaric heat capacity of the ideal gas is required. For a reliable description of caloric properties, speed of sound or heat capacity measurements must also be considered. Data were taken from original literature sources and transferred into SI units as well as to the international temperature scale ITS-90. Due to the challenging properties of hydrogen chloride, the available database is rather restricted. In case of the homogeneous density, only four references are available, whereas no speed of sound or isobaric heat capacity data were published prior to this work. Thus, speed of sound measurements for the liquid phase were carried out here. The application of these data to the present fit yields a significant improvement of the description of the caloric properties.

2 Speed of Sound Measurements

Speed of sound measurements were performed for hydrogen chloride, which was purchased from Air Liquide with a given purity in terms of volume fraction of better than 99.8 % and a content of inert gases of < 0.2 %.[2] It was delivered in a gas cylinder (6 kg) at a vapor pressure of about 4.25 MPa at 293.15 K and was used without any further purification.

The pulse-echo technique with a classical double path length type sensor was applied as measurement principle in combination with pulse design and signal enhancement.[3] Here, a burst of sound waves with the frequency f = 8 MHz, emitted by an excited quartz crystal, propagates through the fluid over the path lengths l_1 = 20 mm and l_2 = 30 mm, is reflected and propagates back to the quartz crystal that also acts as a receiver for the echoes, cf. Figure 1. The speed of sound, neglecting dispersion and diffraction effects, is given by the ratio of path length difference and propagation time

$$w = \frac{2\left(l_2 - l_1\right)}{\Delta t} = \frac{\Delta l}{\Delta t}. \tag{1}$$

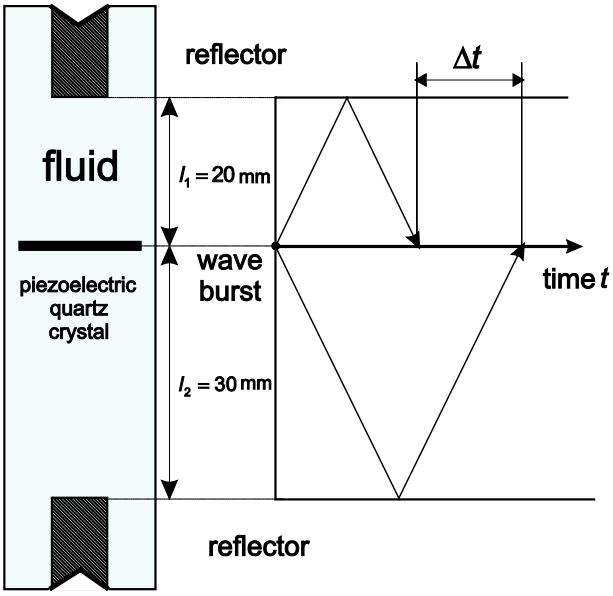

Figure 1. Principle of the pulse-echo technique, where the propagation time difference Δt between the received echoes of a wave burst is a consequence of two different path lengths l_1 and l_2.

Unlike measurements of other fluids that are typically carried out along isotherms, quasi-isochoric measurements were performed here to avoid filling and release processes as much as possible. Upon changes of the state point, the measuring cell underwent expansion or contraction so that its volume was not constant. However, both temperature and pressure of the fluid were measured so that the sampled speed of sound was associated with these two properties.

For filling the measuring cell with fluid, the HCl gas cylinder was mounted upside down to sample the liquid phase and was connected to the measuring cell. After its evacuation, the measuring cell was filled at room temperature by opening the cylinder valve.

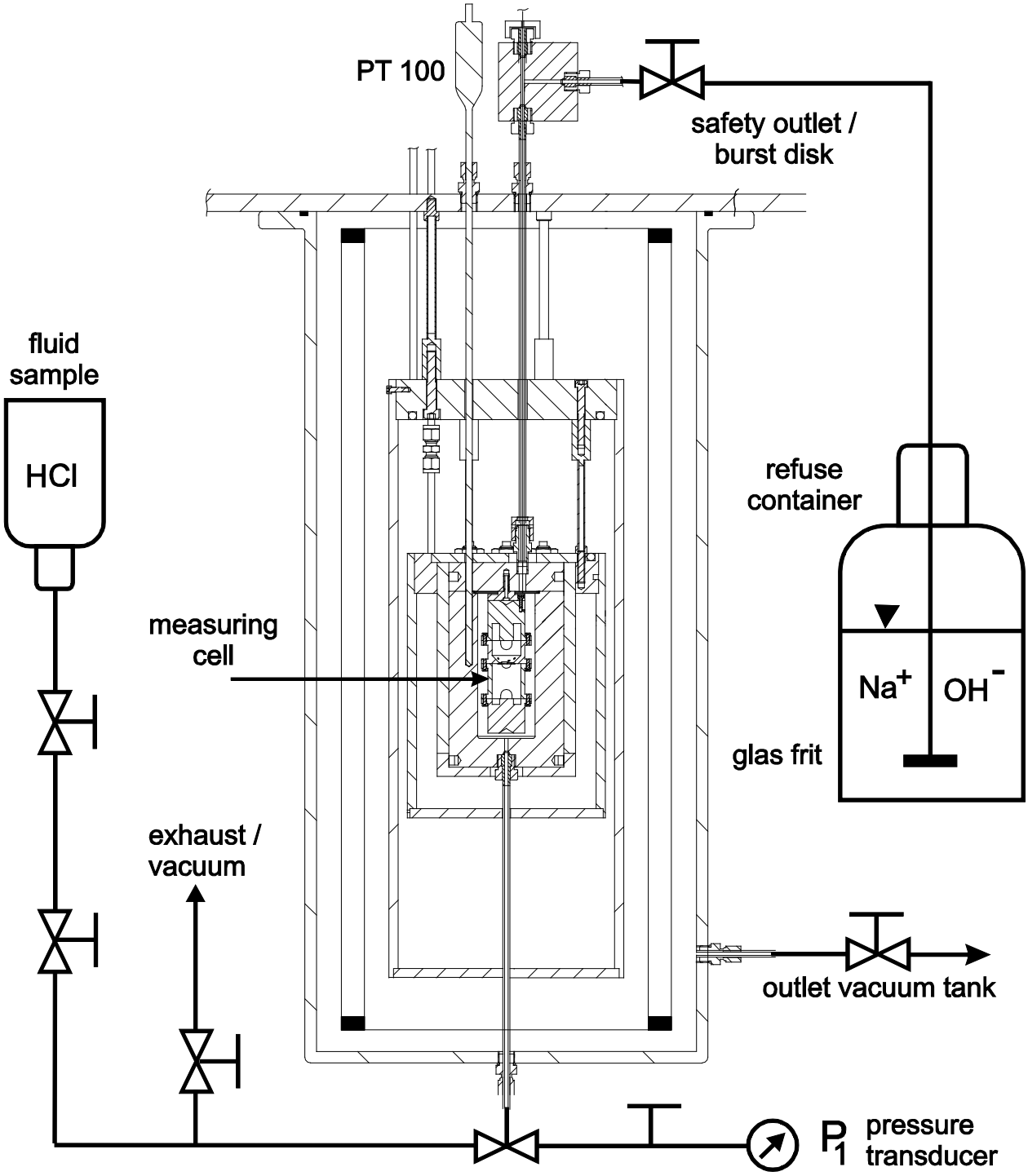

Figure 2. Hydraulic set up of the speed of sound measurement apparatus. The measuring cell was filled with liquid HCl and released HCl was neutralized by sodium hydroxide solution in a refuse container.

Then, the measuring cell was cooled down to 218 K to measure the first state point, which was a saturated liquid. Pressure transducer readings during that cooling indicated phase separation by a crossover in the temperature dependence of the pressure. Without changing the mass of HCl, the measurement cell was heated up by 5 K to attain another state point in a stepwise manner until a pressure of 40 MPa was reached, which was the maximum pressure that was allowed due to safety considerations. As a consequence of these stepwise temperature changes at roughly constant volume, homogeneous state points were attained. Two more quantities of HCl in the measuring cell were prepared by refilling at 273 K and 260 K. Another five additional quantities were achieved by partial release of HCl (at 300 K, 309 K, 324 K, 373 K, 400 K) through a valve to a glass frit that was in a washing bottle, where the HCl gas was neutralized by a sodium hydroxide solution, cf. Figure 2. As a safety indicator, phenolphthalein was used, signalizing chemical equilibrium and the necessity to renew the alkaline solution.

Speed of sound measurements were carried out for 11 saturated liquid states between 218 K and 273 K as well as along eight quasi-isochors in a temperature range of 218 K to 479 K up to a pressure of 40 MPa, cf. Figure 3.

The applied pressure transducer (Honeywell TJE), with a measuring range of up to 200 MPa and an uncertainty of 0.1 % with respect to its full scale, had a maximum absolute uncertainty of 0.2 MPa. This pressure uncertainty $u(p)$ has the largest impact at low temperatures because of the high derivative of the speed of sound with respect to the pressure at constant temperature at such states. Therefore, its usage, especially at low pressure, was not optimal. However, due to the challenging properties of hydrogen chloride, it was not possible to replace the pressure transducer by a more accurate device.

The overall expanded speed of sound measurement uncertainty $U(w)$ is composed of the relevant contributions due to standard uncertainties of temperature $u(T)$ and pressure measurements $u(p)$, as well as the uncertainty of the path length difference $u(l)$ and the uncertainty of the resolution of the time measurement $u(t)$

$$U(w) = k\sqrt{\left(\left(\frac{\partial w}{\partial T}\right)_{p,l,t} u(T)\right)^2 + \left(\left(\frac{\partial w}{\partial p}\right)_{T,l,t} u(p)\right)^2 + \left(\left(\frac{\partial w}{\partial l}\right)_{p,T,t} u(l)\right)^2 + \left(\left(\frac{\partial w}{\partial t}\right)_{p,l,T} u(t)\right)^2} \,. \tag{2}$$

According to the error propagation law, the total uncertainty increased up to 2.6 % for measurements at a density of ρ = 20 mol·dm^{-3} and pressures below 11 MPa. For the remaining state points, the total uncertainty varied between 0.1 % and 1.5 %. Table 1 provides the present experimental data together with their combined expanded uncertainties (k = 2) in numerical form. Note that the sample purity was not considered in this estimate.

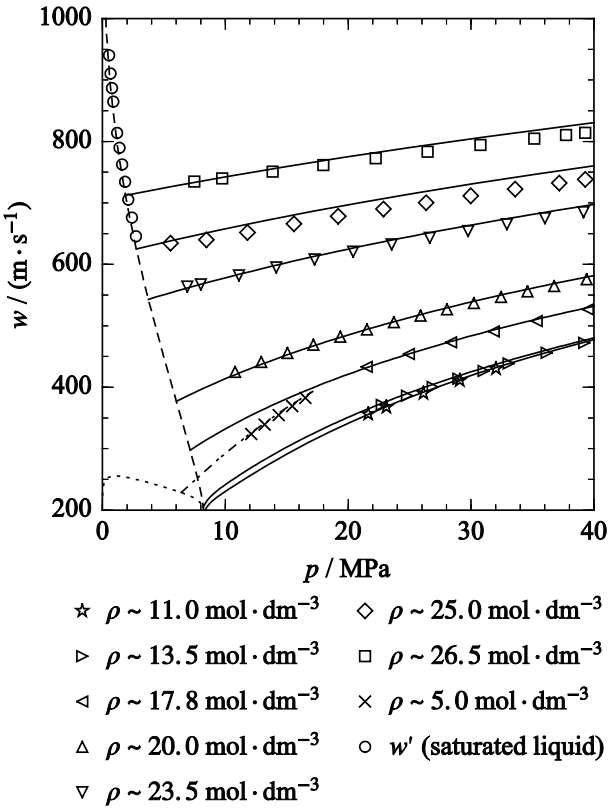

Figure 3. Speed of sound as function of pressure for hydrogen chloride. The experimental data, as depicted by symbols, are only roughly isochoric, e.g. because of measuring cell expansion effects. The corresponding liquid isochors calculated from the present equation of state are shown as solid curves, the saturated liquid and vapor lines are represented by dashed and dotted curves, and the vapor isochor ρ = 5 mol·dm^{-3} is given by the dashed-dotted curve.

Table 1. Experimental speed of sound data w at temperature T and pressure p (vapor pressure p_v). The combined expanded uncertainties $U(w)$ ($k = 2$) were calculated on the basis of the individual uncertainties for pressure $U(p) = 0.4$ MPa, temperature $U(T) = 0.1$ K, propagation length $U(l) = 14$ μm, and time difference $U(t) = 0.004$ μs.

p / MPa	T / K	w / (m·s^{-1})	$U(w)$ / (m·s^{-1})	p / MPa	T / K	w / (m·s^{-1})	$U(w)$ / (m·s^{-1})
Saturated liquid				20 mol·dm^{-3}			
p_v	218.3	940	3	10.8	320.0	425	11
p_v	224.3	910	3	12.9	325.0	441	9
p_v	229.2	887	3	15.1	330.0	456	8
p_v	233.1	865	3	17.2	335.0	469	7
p_v	243.0	814	3	19.3	340.0	482	7
p_v	248.0	790	4	21.5	345.0	494	6
p_v	252.9	762	4	23.7	350.0	506	6
p_v	258.0	734	4	25.9	355.0	517	5
p_v	263.0	705	4	28.0	360.0	527	5
p_v	268.0	676	5	30.2	365.0	537	5
p_v	273.0	646	5	32.4	370.0	547	4
				34.6	374.9	556	4
~26.5 mol·dm^{-3}				36.8	379.9	565	4
7.5	267.0	735	4	39.4	385.9	575	4
9.7	269.9	740	4				
13.9	274.8	751	4	~17.8 mol·dm^{-3}			
18.0	279.8	761	3	21.5	359.9	433	7
22.2	284.8	773	3	24.9	369.9	454	6
26.5	289.8	783	3	28.4	379.9	473	5
30.8	294.8	794	3	31.8	389.9	491	4
35.1	300.0	805	3	35.3	399.9	508	4
37.7	303.1	810	3	39.5	411.9	526	4
39.3	305.0	814	3				
				~13.5 mol·dm^{-3}			
~25 mol·dm^{-3}				22.7	394.9	371	5
5.5	279.8	634	5	24.8	404.9	386	4
8.5	284.8	640	5	26.9	414.9	400	4
11.8	289.7	652	5	29.0	424.9	414	4
15.6	294.8	666	4	31.0	434.9	426	3
19.2	299.8	678	4	33.1	444.9	438	3
22.9	305.0	690	4	36.1	460.0	456	3
26.3	310.0	700	4	39.2	474.9	472	3
30.0	315.0	712	3				
33.6	320.0	722	3	~11 mol·dm^{-3}			
37.2	325.0	732	3	21.6	409.9	356	4
39.3	328.0	738	3	23.1	419.9	368	3
				26.1	439.9	390	3
~23.5 mol·dm^{-3}				29.1	459.9	411	3
6.9	292.9	564	7	32.0	479.9	430	2
8.0	295.0	567	7				
11.1	300.0	582	6				

p / MPa	T / K	w / (m·s^{-1})	$U(w)$ / (m·s^{-1})		p / MPa	T / K	w / (m·s^{-1})	$U(w)$ / (m·s^{-1})
14.2	305.0	595	5		~5 mol·dm^{-3}			
17.3	310.0	608	5		12.1	399.9	324	1
20.4	315.0	621	5		13.2	419.9	339	1
23.5	320.0	632	4		14.3	439.9	355	1
26.6	325.0	643	4		15.5	460.0	369	1
29.8	330.0	654	4		16.5	479.9	383	1
32.9	335.0	665	4					
36.0	340.0	675	3					
39.2	345.0	685	3					

3 Equation of State

The present equation of state is expressed in terms of the molar Helmholtz energy a, which is reduced by the temperature and the universal gas constant R = 8.3144598 J·mol^{-1}·K^{-1}

$$\alpha(\tau,\delta)=\frac{a(T,\rho)}{RT}, \tag{3}$$

with reduced density $\delta = \rho/\rho_c$ and inverse reduced temperature $\tau = T_c/T$ as independent variables. Furthermore, it is separated into an ideal part α^o representing the behavior of a hypothetical ideal gas and a residual part α^r taking the intermolecular interactions into account

$$\alpha(\tau,\delta)=\alpha^{o}(\tau,\delta)+\alpha^{r}(\tau,\delta). \tag{4}$$

The ideal gas behavior can be obtained from a correlation for the isobaric heat capacity of the ideal gas on the basis of the Planck-Einstein equation

$$\frac{c_p^o}{R}=n_0+\sum_{i=1}^{3}m_i\left(\frac{\theta_i}{T}\right)^2\frac{\exp(\theta_i/T)}{\left(\exp(\theta_i/T)-1\right)^2} \tag{5}$$

by means of a two-fold integration with respect to the reciprocal reduced temperature

$$\alpha^{o}(\tau,\delta)=c^{II}+c^{I}\tau+c_0\ln(\tau)+\ln(\delta)+\sum_{i=1}^{3}m_i\ln\left(1-\exp(-\theta_i/T_c\,\tau)\right). \tag{6}$$

The integration constants c^I and c^{II} can be chosen arbitrarily. In this work, the ideal gas reference state was chosen for their specification. Its density was calculated with the help of the thermal equation of state of the ideal gas $\rho_0 = p_0/(RT_0)$ with the reference temperature T_0 = 298.15 K and the reference pressure p_0 = 0.101325 MPa. The default reference values for the corresponding entropy s_0^o and enthalpy h_0^o of the ideal gas were set to be zero. The resulting integration constants and the parameters of the Planck-Einstein terms according to Eq. (6) are listed in Table 2.

Table 2. Parameters of the ideal part of the present equation of state (cf. Eq. (6)). c^I and c^{II} are the integration constants, which define the reference point for caloric properties.

i	1	2	3	c_0	c^I	c^{II}
m_i	0.0033327	0.935243	0.209996	2.5	4.0257768311	−4.069044527
θ_i / K	300	4000	6300			

For the parametrization of the ideal gas heat capacity equation, two different references were available. In both publications, this property was not measured but evaluated by means of statistical mechanics. Comparisons of these data with the present equation of state are illustrated in Figure 4. The isobaric heat capacity data of the ideal gas published by Austin[4] in 1932 are the first in the literature for hydrogen chloride. He reported ideal gas heat capacity data for different hydrogen halides, including hydrogen chloride, and took the underlying parameters from Salant and Sandow.[5]

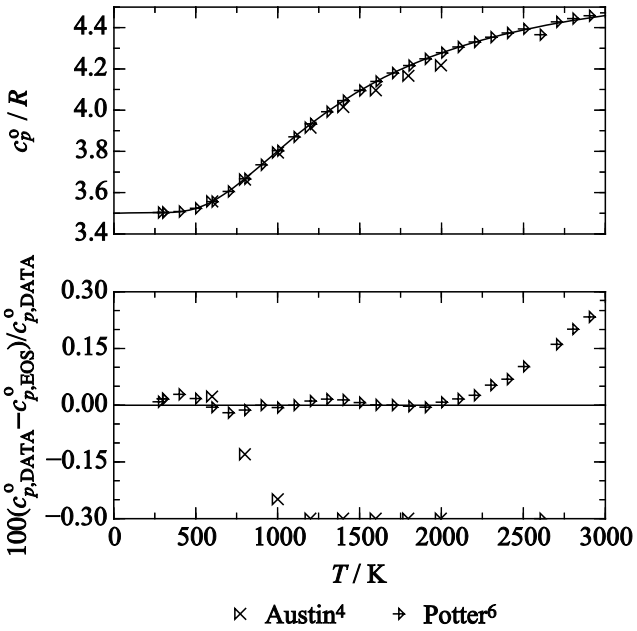

Figure 4. Representation of the isobaric heat capacity of the ideal gas with the present equation of state.

In the following decades, the methods to determine ideal gas heat capacity data from statistical mechanics became more accurate. Potter[6] published his data in 1959 together with ideal gas heat capacity data for molecular chlorine and fluorinated chlorine. Spectroscopic data were taken from the literature[7,8] and the underlying calculations follow the same route as those for chlorine.[6] For hydrogen chloride, no experiments are available for verification, but for chlorine, there are ideal gas heat capacity data derived from speed of sound measurements of Hurly.[9] Between $T = 260$ K and 420 K, these data agree with Potter's[6] calculations within approximately 0.05 %. Therefore, the approach of Potter[6] was assumed to be more trustworthy and his data were applied to the present fit. The equation can reproduce these data within 0.03 % for $T < 2000$ K; deviations increase for higher temperatures, which is far beyond the range of validity of the equation of state. Because these data are probably less accurate than they were fitted here, the expected uncertainty of the present equation for the ideal gas heat capacity is estimated to be 0.1 %.

The residual part of the equation of state consists of five polynomial, five exponential, and five Gaussian bell-shaped terms, cf. Eq. (7). The adjustable parameters n_i, t_i, d_i, p_i, η_i, β_i, γ_i, and ε_i were determined by means of a non-linear fitting algorithm developed at the National Institute of Standards and Technology.[10,11] Similar to other modern equations of state, not only experimental data, but also several constraints were applied to the fitting procedure to ensure a correct physical behavior in regions where no experimental data are available. For further information, see e.g. Refs.[11–15] The numerical values of the equation parameters are listed in Table 3. Test values for computer implementation are provided in Table 4**Fehler! Verweisquelle konnte nicht gefunden werden.**.

$$\begin{aligned}\alpha^{\mathrm{r}}(\tau,\delta) &= \alpha^{\mathrm{r}}_{\mathrm{Pol}}(\tau,\delta) + \alpha^{\mathrm{r}}_{\mathrm{Exp}}(\tau,\delta) + \alpha^{\mathrm{r}}_{\mathrm{GBS}}(\tau,\delta) \\ &= \sum_{i=1}^{5} n_i \delta^{d_i} \tau^{t_i} + \sum_{i=6}^{10} n_i \delta^{d_i} \tau^{t_i} \exp\left(-\delta^{p_i}\right) \\ &+ \sum_{i=11}^{15} n_i \delta^{d_i} \tau^{t_i} \exp\left(-\eta_i (\delta - \varepsilon_i)^2 - \beta_i (\tau - \gamma_i)^2\right).\end{aligned} \tag{7}$$

Table 3. Parameters of the residual part of the present equation of state (cf. Eq. (7)).

i	n_i	t_i	d_i	p_i	η_i	β_i	γ_i	ε_i
1	$1.952802\cdot10^{-2}$	1.000	4	-				
2	$1.926809\cdot10^{+0}$	0.553	1	-				
3	$-2.835744\cdot10^{+0}$	1.037	1	-				
4	$-2.276121\cdot10^{-1}$	0.817	2	-				
5	$8.843713\cdot10^{-2}$	0.378	3	-				
6	$-2.433471\cdot10^{+0}$	1.523	1	2				
7	$-2.636625\cdot10^{-1}$	2.656	3	2				
8	$6.307008\cdot10^{-1}$	1.338	2	1				
9	$-6.382638\cdot10^{-1}$	2.828	2	2				
10	$-6.851438\cdot10^{-3}$	0.750	7	1				
11	$7.363661\cdot10^{+0}$	0.644	1	-	1.141	0.95	1.56	0.855
12	$-1.262993\cdot10^{+0}$	2.892	1	-	1.162	0.92	1.14	0.910
13	$-6.539739\cdot10^{-3}$	0.760	3	-	34.60	1550	1.06	0.942
14	$-8.752692\cdot10^{-1}$	1.323	2	-	1.175	1.2	0.94	0.702
15	$-3.224835\cdot10^{+0}$	0.693	2	-	0.990	0.89	1.25	0.487

Table 4. Test values for computer implementation. Listed are temperature T, density ρ, pressure p, enthalpy h, entropy s, speed of sound w, and Helmholtz energy a. The number of digits does not refer to the accuracy of the equation of state.

T / K	ρ / (mol·dm^{-3})	p / MPa	h / (J·mol^{-1})	s / (J·mol^{-1}·K^{-1})	w / (m·s^{-1})	a / (J·mol^{-1})
180	34	$3.20901855\cdot10^{+1}$	$1.43888365\cdot10^{+2}$	$-4.43856331\cdot10^{+0}$	$1.24521167\cdot10^{+3}$	$-9.99224087\cdot10^{-1}$
180	0.04	$5.86755086\cdot10^{-2}$	$1.60017182\cdot10^{+4}$	$8.94473371\cdot10^{+1}$	$2.37450444\cdot10^{+2}$	$-1.56569018\cdot10^{+3}$
300	25	$2.05806246\cdot10^{+1}$	$7.23911135\cdot10^{+3}$	$2.72001575\cdot10^{+1}$	$6.91262823\cdot10^{+2}$	$-1.74416090\cdot10^{+3}$
300	3	$4.70517077\cdot10^{+0}$	$1.63991807\cdot10^{+4}$	$6.01776839\cdot10^{+1}$	$2.43922254\cdot10^{+2}$	$-3.22251469\cdot10^{+3}$
400	18	$3.61071944\cdot10^{+1}$	$1.37983760\cdot10^{+4}$	$4.40061792\cdot10^{+1}$	$5.15047201\cdot10^{+2}$	$-5.81005088\cdot10^{+3}$

4 Comparison with Literature Data

The representation of the available experimental data with the present equation of state was analyzed by means of a percentage deviation according to

$$\Delta X = 100 \frac{x_{\mathrm{DATA}} - x_{\mathrm{EOS}}}{x_{\mathrm{DATA}}}, \tag{8}$$

and the average absolute relative deviation

$$\mathrm{AAD} = \frac{1}{N} \sum_{i=1}^{N} \left| \Delta X_i \right|, \tag{9}$$

where x is a given thermodynamic property at a certain state point and N is the number of data points. For a first overview about the quality of the data, the AAD for every literature reference is listed in Tables 5 and 6. For a better assessment of comprehensive data sets, the AAD was separated into different state regions: gas, liquid, critical region, and supercritical region considering three density ranges (LD, MD, HD) as given in Table 5. The thermal vapor-liquid equilibrium data are categorized into low (LT), medium (MT), and high temperature (HT) ranges in Table 6.

In the figures discussed below, the equation of Thol *et al.*[16] is also shown. It was developed as a part of a work on a new generalized functional form for weakly associating fluids and, therefore, it was not optimized in a fluid-specific way. It exhibits some issues, e.g., a poor representation of caloric properties and an incorrect critical point. With the present equation of state, these problems are solved.

Table 5. Average absolute relative deviation (AAD) of experimental data in the homogeneous region calculated with the present equation of state, where N is the number auf data points. For the $p\rho T$ data, deviations are calculated in terms of density except for the critical region where pressure deviations are given.

					AAD / %						
Author	Year	N	T_{min} - T_{max} / K	p_{min} - p_{max} / MPa	gas	liq.	crit. reg.a	LD[a]	MD[a]	HD[a]	Over-all
c_p^o											
Austin[4]	1932	8	600 - 1997	$p \rightarrow 0$	0.65	-	-	-	-	-	0.65
Potter[6]	1959	50	273 - 5013	$p \rightarrow 0$	0.37	-	-	-	-	-	0.37
$p\rho T$											
Dorsman[17]	1908	212	293 - 326	3.1 - 10	1.43	1.1	0.26	1.2	2.5	-	1.3
Franck *et al.*[18]	1962	273	333 - 674	5.7 - 204	-	-	4.0	1.5	4.8	0.66	2.7
Nunes da Ponte & Staveley[19]	1981	32	188 - 244	1.4 - 5	-	0.34	-	-	-	-	0.34
Thomas[20]	1962	38	273 - 348	3.5 - 19	-	0.14	0.48	-	0.44	0.43	0.28
w											
This work	2017	83	224 - 480	0.0 - 40	-	0.29	-	0.48	0.25	0.15	0.21
c_p											
Chihara & Inaba[21]	1976	2	161 - 165	p_v	-	4.2	-	-	-	-	4.2
Clusius[22]	1929	6	163 - 174	p_v	-	0.28	-	-	-	-	0.28

					AAD / %						
			T_{min} - T_{max}	p_{min} - p_{max}			crit.				Over-
Author	Year	*N*	/ K	/ MPa	gas	liq.	reg.a	LD[a]	MD[a]	HD[a]	all
Eucken & Karwat[23]	1924	9	168 - 189	p_v	-	4.1	-	-	-	-	4.1
Giauque & Wiebe[24]	1928	5	163 - 186	p_v	-	3.4	-	-	-	-	3.4
Grosh *et al.*[25]	1965	4	158 - 189	p_v	-	3.8	-	-	-	-	3.8
c_v											
Franck *et al.*[18]	1962	83	333 - 574	7.0 - 33	-	0	15.4	4.6	7.7	5.5	7.1
h_{vap}											
Giauque & Wiebe[24]	1928	2	188.11	p_v	0.21	-	-	-	-	-	0.21
B											
Franck *et al.*[18]	1962	22	372 - 574	p_v	8.6	-	-	-	-	-	8.6
Nunes da Ponte & Staveley[19]	1981	11	159 - 241	p_v	12.8	-	-	-	-	-	12.8
Schramm & Leuchs[26]	1979	13	190 - 480	p_v	5.3	-	-	-	-	-	5.3
Wormald & Massucci[27]	1997	7	210 - 371	p_v	10.4	-	-	-	-	-	10.4

[a] Supercritical fluid: LD: $\rho/\rho_c \leq 0.6$; MD: $0.6 \leq \rho/\rho_c \leq 1.5$; HD: $\rho/\rho_c > 1.5$

Table 6. Average absolute relative deviation (AAD) of experimental vapor-liquid equilibrium data calculated with the present equation of state, where *N* is the number of data points..

				AAD / %			
Author	Year	*N*	T_{min} - T_{max} / K	LT[a]	MT[a]	HT[a]	overall
p_v							
Ashley & Brown[28]	1954	4	213 - 244	-	0.15	-	0.15
Briner & Cardoso[29]	1908	4	303 - 319	-	1.6	-	1.6
Calado *et al.*[30]	1975	3	159 - 196	0.48	0.58	-	0.51
Calado *et al.*[31]	1978	1	195.43	-	0.58	-	0.58
Chihara & Inaba[21]	1976	4	160 - 166	0.29	-	-	0.29
Dorsman[17]	1908	26	293 - 325	-	0.56	0.15	0.43
Faraday[32]	1845	26	199 - 278	-	1.7	-	1.7
Florusse & Peters[33]	2002	10	283 - 325	-	0.89	0.099	0.57
Franck *et al.*[18]	1962	5	303 - 324	-	0.23	0.37	0.26
Giauque & Wiebe[24]	1928	9	164 - 196	0.49	0.38	-	0.48
Giles & Wilson[34]	2000	2	258 - 279	-	0.48	-	0.48
Gillespie *et al.*[35]	1985	3	192 - 267	2.0	0.68	-	1.5
Haase *et al.*[36]	1963	1	298.14	-	1.2	-	1.2
Henderson *et al.*[37]	1986	27	159 - 220	0.44	0.24	-	0.40
Henglein[38]	1923	1	161.02	0.50	-	-	0.49
Henning & Stock[39]	1921	4	164 - 187	0.16	-	-	0.16
Karwat[40]	1926	1	159.36	2.7	-	-	2.7
Ladenburg & Kruegel[41]	1900	1	190.09	12.0	-	-	12.0
Lobo & Staveley[42]	1984	1	182.33	0.34	-	-	0.34
Lobo *et al.*[43]	1985	2	159 - 174	0.22	-	-	0.22
Maass & McIntosh[44]	1914	26	160 - 190	4.8	-	-	4.8
Mahler *et al.*[45]	1994	1	263.15	-	0.51	-	0.51
Senra *et al.*[46]	2002	2	159 - 183	0.35	-	-	0.35
Senra *et al.*[47]	2005	2	159 - 183	0.29	-	-	0.29

				AAD / %			
Author	Year	N	T_{min} - T_{max} / K	LT[a]	MT[a]	HT[a]	overall
Steele *et al.*[48]	1906	9	163 - 193	11.0	-	-	11.0
Stock[49]	1923	32	162 - 194	0.063	-	-	0.063
Stock *et al.*[50]	1921	24	165 - 189	0.10	-	-	0.10
Thomas[20]	1962	9	273 - 322	-	0.68	0.093	0.61
Washburn *et al.*[51]	1926	6	203 - 244	-	0.56	-	0.56
Wilding *et al.*[52]	1987	2	243 - 274	-	1.4	-	1.4
Wilding *et al.*[53]	1996	2	233 - 274	-	0.50	-	0.50
Wilding *et al.*[54]	2002	2	248 - 274	-	0.55	-	0.55
Wilson & Wilding[55]	1994	4	203 - 274	-	1.4	-	1.4
ρ'							
Dorsman[17]	1908	9	293 - 325	-	1.5	0.31	1.1
Franck *et al.*[18]	1962	5	303 - 324	-	1.2	1.9	1.4
Henderson *et al.*[37]	1986	26	162 - 237	0.058	0.14	-	0.094
Kanda[56]	1937	10	160 - 183	0.83	-	-	0.83
Lobo & Staveley[42]	1984	1	182.33	0.038	-	-	0.038
Rupert[57]	1909	17	223 - 325	-	0.43	9.4	1.5
Steele *et al.*[48]	1906	9	163 - 193	0.61	-	-	0.61
Thomas[20]	1962	12	274 - 320	-	0.15	0.21	0.15
ρ''							
Dorsman[17]	1908	9	293 - 325	-	1.6	2.3	1.8
Franck *et al.*[18]	1962	5	303 - 324	-	4.8	11.0	6.0
Rupert[57]	1909	17	223 - 325	-	5.4	29.0	8.1
Steele *et al.*[48]	1906	9	163 - 193	12.0	-	-	12.0

[a] LT: $T/T_c \leq 0.6$; MT: $0.6 \leq T/T_c \leq 0.98$; HT: $T/T_c > 0.98$

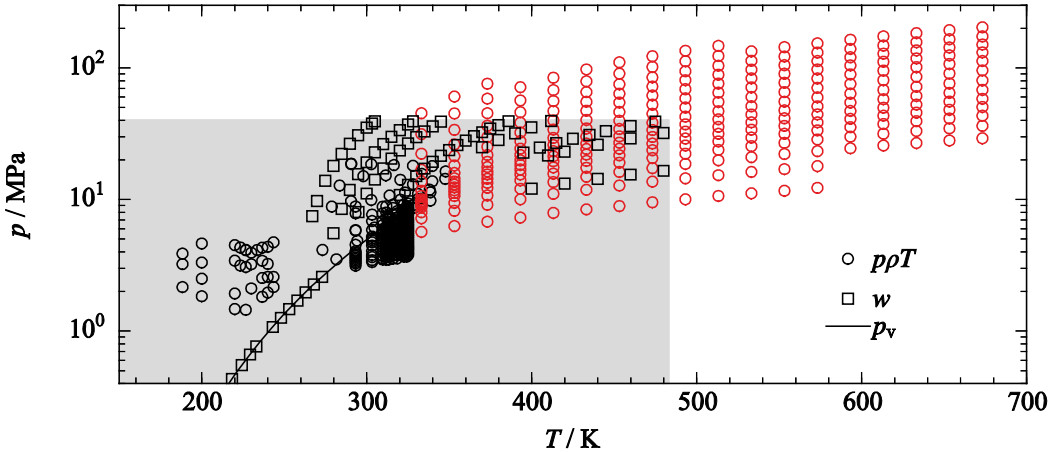

Figure 5. p,T-diagram including the vapor pressure curve (p_v) and available homogeneous density ($p\rho T$) and speed of sound (w) data. The density data of Franck *et al.*[18] are depicted by red circles because they were not taken into account during the fitting procedure. The grey surface marks the range of validity of the present equation of state based on the remaining experimental data.

The available homogeneous density and speed of sound data are illustrated in a p,T-diagram in Figure 5. For the development of the equation of state, these data are used together with the vapor-liquid equilibrium and second virial coefficient data listed in Tables 5 and 6. However,

the data of Franck *et al.*[18] have large experimental uncertainties and, thus, were not applied to the fit. When omitting these data, Figure 5 shows that the database is rather limited. The temperature range is T = 159.07 K to 480 K with pressures up to p = 40 MPa. Taking the less accurate data set of Franck *et al.*[18] into account, the maximum temperature and pressure are T_{max} = 670 K and p_{max} = 200 MPa, respectively. The critical temperature was taken from Thomas[20] and slightly adjusted for a better representation of the data in the critical region. The resulting value is T_c = 324.68 K. The critical density ρ_c =11.87 mol·dm^{-3} was determined during the fit and lies between the two values available in the literature (Grosh *et al.*[25]: 11.27 mol·dm^{-3} and Franck *et al.*[18]: 12.34 mol·dm^{-3}). The critical pressure p_c = 8.3135 MPa was calculated from the present equation of state. Based on the triple point temperature T_{tp} = 159.07 K published by Senra *et al.*,[46] the according saturated liquid density $\rho_{tp,liq}$ = 34.4 mol·dm^{-3} was calculated by extrapolation of the saturated liquid line. For the conversion to specific units, the molar mass M = 36.4609 g·mol^{-1} of Wieser and Berglund[58] was adopted.

4.1 Homogeneous Density and Thermal Virial Coefficients

The homogeneous density was investigated by Dorsman,[17] Franck *et al.*,[18] Nunes da Ponte and Staveley,[19] and Thomas.[20] Percentage deviations with respect to the present equation of state and the equation of Thol *et al.*[16] are presented in Figure 6. The gaseous region was only investigated by Dorsman[17] and his data are represented within 1.5 %. These data were only published in his dissertation in 1908, which is not available. Therefore, information on the measurement procedure or the experimental uncertainty is not available. Because there are no other experimental data, this deviation is assumed to be the uncertainty of the equation in the gaseous region, but for a reliable statement new data have to be measured.

The liquid region was studied by Dorsman[17] (AAD = 1.1 %), Nunes da Ponte and Staveley[19] (AAD = 0.34 %), and Thomas[20] (AAD = 0.14 %). Most of these data can be reproduced within 1 %. The large AAD of Dorsman[17] is caused by two outliers at T = 313.33 K. Removing those two values from the statistical analysis leads to an AAD = 0.48 % in the liquid region. The data of Thomas[20] are located in the same temperature and pressure range as Dorsman's[17] data and are represented within 0.5 % for densities below 20 mol·dm^{-3} and even within 0.1 % for higher densities. During his experiment, Dorsman[17] prepared a known amount of fluid in a pressure vessel with a U-shaped pressure transmitter filled with mercury. The volume of the vessel was kept constant and the equilibrium pressure was measured while varying the temperature. The volume of the working cell was determined with the help of a well-known mass of mercury and carbon dioxide. Both measurements agreed within 0.1 % with respect to the mass. The pressure was measured with an uncertainty of 0.1 %, whereas the temperature was maintained within 0.01 K. The resulting combined expanded uncertainty (k = 2) is 0.2 % to 1.8 % in terms of the density, where the low value corresponds to high

pressures. The final results were smoothed. This correction and the sample purity of 99.7 % are additional contributions of the experimental uncertainty, which were not considered in his analysis. The data are reproduced with the present equation within the experimental uncertainty, although the specified experimental uncertainty is probably too low.

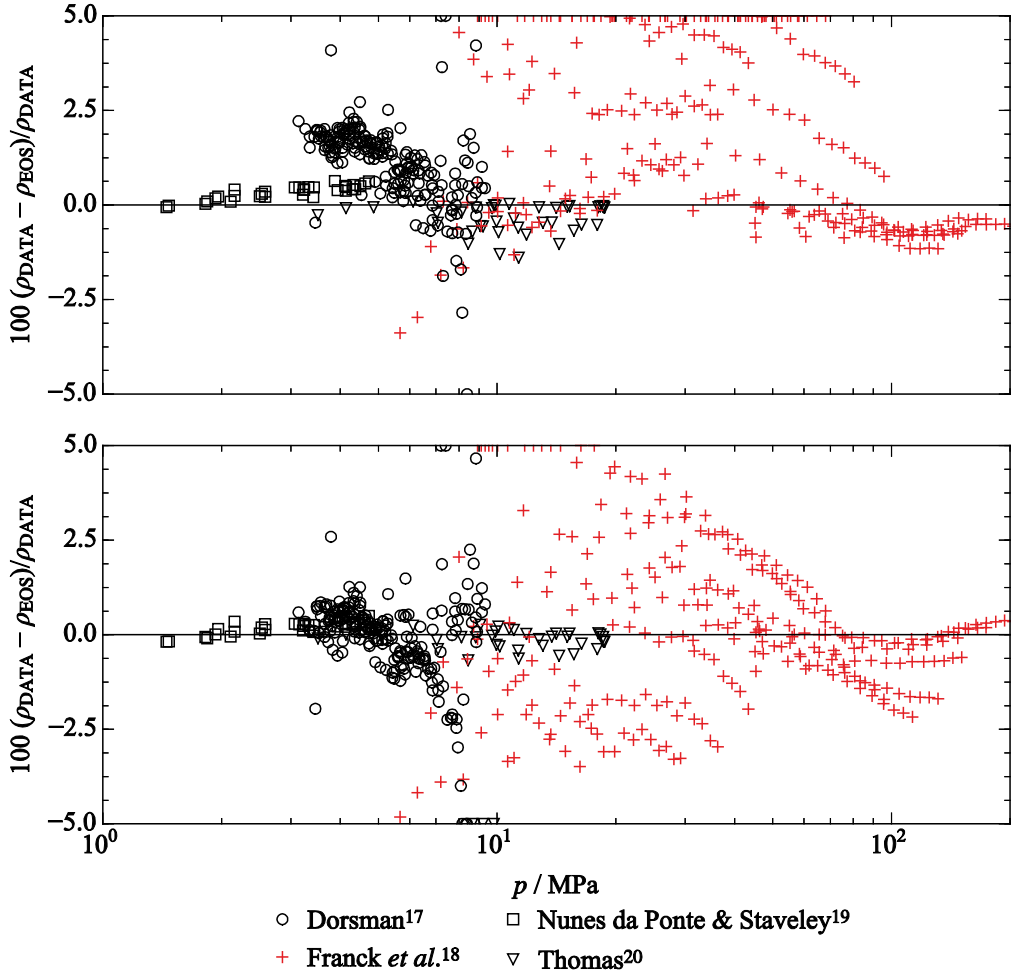

Figure 6. Percentage deviation of homogeneous density data from the present equation of state (top) and the equation of Thol *et al.*[16] (bottom).

The measurements of Nunes da Ponte and Staveley[19] were carried out with a pressure cell as described by Nunes da Ponte *et al.*[59] The uncertainties given in their paper (ΔT = 0.01 K, Δp = 0.1 MPa, and $\Delta \rho$ = 0.1 %) yield a combined expanded uncertainty of 0.22 % in density (k = 2). The present equation of state deviates from these data by approximately 0.5 %. Deviations increase with increasing pressure, which is most probably due to the limitations of the utilized apparatus that was primarily designed to study compressible gases at room temperature. Therefore, the maximum pressure was restricted to 5 MPa. Measurements for nitrogen and methane,[59] which were done with the same apparatus, are reproduced within 0.3 % by the reference equations of state of Span *et al.*[60] and Setzmann and Wagner.[61] Therefore, the uncertainty of the measurements for hydrogen chloride is assumed here to be at least 0.3 % and representing them within 0.5 % seems to be reasonable. Based on the data of Nunes da Ponte

and Staveley[19] and Thomas,[20] the expected uncertainty of the present equation of state is estimated to be 0.5 % in terms of the density in the liquid state.

The supercritical state was investigated by Franck *et al.*[18] and Thomas.[20] The data of Dorsman[17] were measured along the near-critical isotherm T = 325.13 K, where the average deviation from the present equation of state is 1.5 %, except for two state points in the medium density range. The ten data points of Thomas,[20] which are assumed to be more accurate based on the analysis of the liquid phase, exhibit negative deviations of up to –0.7 %. The most comprehensive dataset in the supercritical region was published by Franck *et al.*[18] In Figures 5 and 6, they are marked in red because they are of questionable accuracy. The measurements were carried out in a calorimeter at temperatures below 473.15 K; higher temperatures were studied in a cylindrical autoclave. The volume of the calorimetric vessel was calibrated with water at 293.15 K. The expansion of the vessel due to temperature and pressure was calculated from the thermal expansion coefficient and the elasticity modulus of the material. No experimental measurements were carried out to verify this approach. The measurement procedure was explained only for the heat capacity so that little information on the pressure measurement is available. Franck *et al.*[18] report that the heat flow between the heated aluminum and the vessel was not completely eliminated so that the experiment was not in equilibrium. Thus, they repeated the measurements and found a reproducibility of the heat capacity of 1 %. For high temperature measurements, the autoclave was filled with hydrogen chloride and heated with a rate of 2 K per minute. Along the autoclave, a temperature gradient of 1 K was observed. The experiment was carried out for increasing temperature first and subsequently for decreasing temperature at the same state points. The measured pressure data differed by up to 0.6 % from each other. The authors decided to consider only the pressure data measured when cooling down the system. Additionally, Franck *et al.*[18] report that their measurement was restricted to T = 673 K because rapid corrosion by hydrogen chloride could not be prevented for higher temperatures. Since corrosion is a creeping process, this problem already had to be incurred below this temperature. Finally, Franck *et al.*[18] correlated an equation to their measurements with a claimed uncertainty of 1 atm (corresponding to 0.05 % to 1.8 % of the experimental pressure). This correlation was used to calculate isotherms and isochors, which are the reported values in their publication. Despite all these issues, the authors claim an uncertainty of only 1.5 %, which is most probably much too low. During the present fitting procedure, it turned out that it is not possible to reproduce these data better than 6 % in density. This seems to be pressure or density dependent because high pressures/densities can be modeled more accurately than low pressures/densities (AAD_{MD} = 4.8 % vs. AAD_{HD} = 0.66 %). The same findings were made by Thol *et al.*[16] when developing the generalized functional form for polar and less associating fluids. The data were thus excluded from the present optimization procedure because it was not possible to reproduce them in a sufficiently accurate manner. Unfortunately, this data set is the only one for pressures above 20 MPa. Therefore, the expected uncertainty of

the present equation of state in the supercritical region is estimated to be 1 % in density. When using it at higher temperatures, pressures, and densities, an uncertainty of at least 6 % has to be accepted.

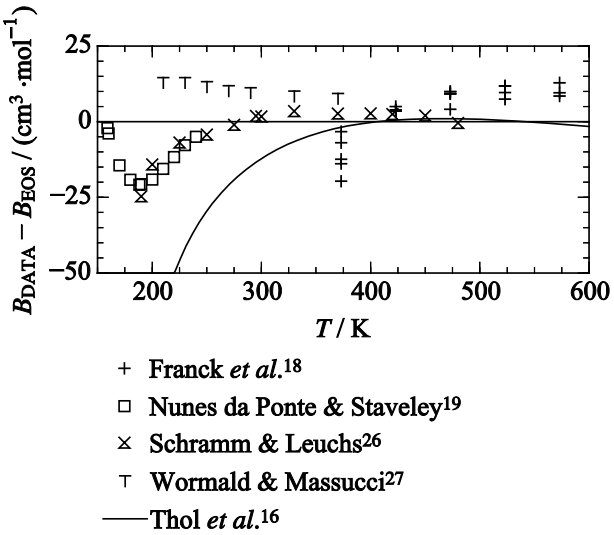

Figure 7. Absolute deviations of second thermal virial coefficient data from the present equation of state.

Comparisons of the present equation of state with second thermal virial coefficient data are shown in Figure 7. Franck *et al.*[18] calculated their values from the equation $pv = RT+Bp$ at five temperatures and several pressures. Because they did not extrapolate to zero pressure/density, they obtained different values at constant temperature and, therefore, these data are of little use. The measurements of Nunes da Ponte and Staveley[19] were carried out in the liquid region and could not be used to determine thermal virial coefficients. Thus, they applied a simple polynomial to the second virial coefficient data of Schramm and Leuchs[26] to interpolate and extrapolate to lower temperatures. This leads to a reasonable description of the data in the temperature overlapping with Schramm and Leuchs. For lower temperatures, deviations exhibit an increasing positive trend, which cannot be verified because no other data are available in this region. The second virial coefficient data of Schramm and Leuchs[26] were measured with two complementary apparatuses, and a sample purity of 99.8 % was reported. A careful analysis of possible error sources was made with a resulting overall uncertainty of 2 cm^3·mol^{-1} to 7 cm^3·mol^{-1}, corresponding to 1.5 % to 10 %. Figure 7 shows that these data are reproduced within this uncertainty for temperatures above 220 K. For lower temperatures, negative deviations rapidly increase. This is in contrast to the most recent data reported by Wormald and Massucci.[27] These data were not measured, but derived from statistical mechanics. A spherical-core Kihara potential[62] with an additional dipole-dipole interaction term was fitted to well-known second thermal virial coefficient data of argon. With a combining rule, the potential parameters of hydrogen chloride were determined such that the theoretical value matches with the experimentally determined excess enthalpy of a hydrogen chloride + argon mixture. This approach overestimates the second virial coefficient of hydrogen chloride by up to 13 cm^3·mol^{-}

[1] with respect to the present equation of state. Based on the data of Schramm and Leuchs[26] and Wormald and Massucci,[27] the uncertainty of the second virial coefficient calculated with the present equation of state is estimated to be 25 cm³·mol^{-1} for T < 300 K and 15 cm³·mol^{-1} for higher temperatures.

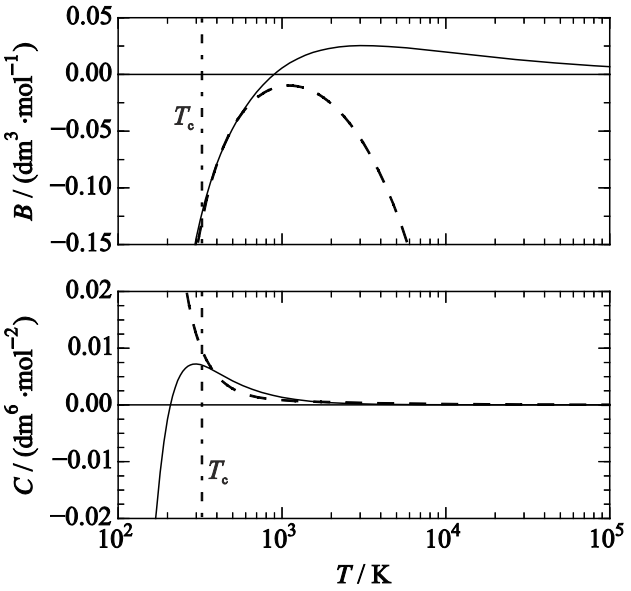

Figure 8. Second and third thermal virial coefficients as a function of temperature calculated with the present equation of state (solid curve) and the equation of Thol *et al.*[16] (dashed curve). T_c indicates the critical temperature.

In addition to comparisons with experimental data, the qualitative behavior of the thermal virial coefficients was analyzed up to very high temperatures. Figure 8 shows a typical trend of the second and third thermal virial coefficient calculated with the present equation of state. Both coefficients exhibit large negative values at low temperatures, pass through a maximum and then approach zero without becoming negative again. As usual, the maximum of the third virial coefficient is located in the vicinity of the critical temperature T_c and it is more distinct than the one for the second virial coefficient. Furthermore, an inflection point above the critical temperature is present. The equation of Thol *et al.*[16] exhibits obvious shortcomings for the second virial coefficient at high temperatures and for the third virial coefficient at low temperatures.

In Figure 9, characteristic ideal curves according to Span and Wagner[63] are depicted, which are closely related to the virial coefficients. These curves are an effective instrument for the analysis of a reliable extrapolation behavior of an equation of state up to high temperatures, pressures, and densities. For the calculation of these curves, density derivatives up to the second order and temperature derivatives are needed. Because no information on these properties except for the first density derivative was available when the equation of Thol *et al.*[16] was developed, the prediction of these curves by the older equation of state is erroneous. Due to new fitting techniques and applying the speed of sound data measured in this work to the fit, all

curves calculated with the present equation of state show a smooth behavior without any unreasonable changes of slope or curvature.

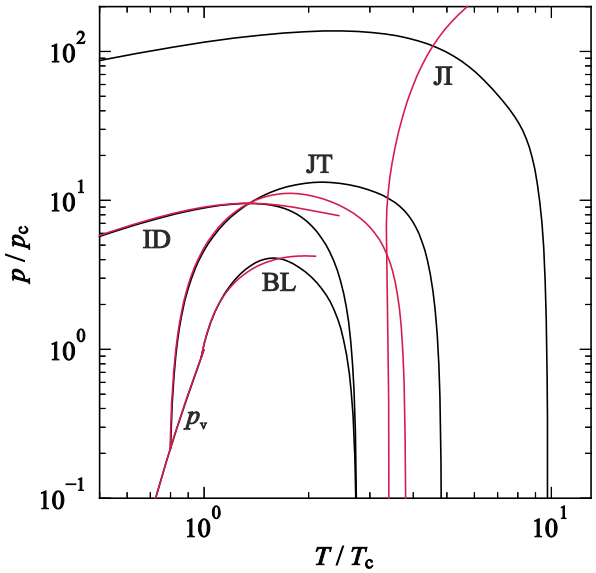

Figure 9. Characteristic ideal curves[63] calculated with the present equation of state (black curves) and the equation of Thol *et al.*[16] (magenta curves) p_v: vapor pressure curve; BL: Boyle curve; ID: ideal curve; JT: Joule-Thomson inversion curve; JI: Joule inversion curve.

4.2 Vapor-Liquid Equilibrium

An overview of the available thermal vapor-liquid equilibrium data is given in Table 6. At first glance, the vapor pressure seems to be comprehensively investigated, cf. Figure 10. However, there are many publications reporting a few state points only. These datasets are not discussed in detail here. For low temperatures ($T < 200$ K), there are data of Giauque and Wiebe,[24] Henning and Stock,[39] Maass and McIntosh,[44] Steele *et al.*,[48] Stock,[49] and Stock *et al.*[50] All of them were published before 1930. The only recent measurements in this region were reported by Calado *et al.*,[30] Chihara and Inaba,[21] and Henderson *et al.*[37] Because the data of Henderson *et al.*[37] are the result of the most comprehensive and most recent measurements, they were applied to the present fitting procedure. The sample was prepared by Calado *et al.*,[31] but no clear statement on its purity is given. To test their apparatus and sample purity, Calado *et al.*[31] measured the triple point pressure with an uncertainty of 0.03 %, which agrees within 0.1 % with the data of several other authors, e.g., Calado *et al.*,[30] Giauque and Wiebe,[24] or Lobo *et al.*[64] During the experiment, they obtained two different datasets. The results of the first series between 161 K and 188 K were more accurate than the second series between 159 K and 220 K, which was traced back to an insufficient thermal equilibrium during the experiment.[37] Therefore, the first series can be reproduced within 0.35 %, while the second series deviates by up to 1.2 % from the present equation of state. However, the second series was still valuable here to partly bridge the gap between these low temperature measurements and the high temperature data of Thomas.[20] In this way, even the old data of Henning and Stock[39] (AAD = 0.16 %), Stock[49] (AAD = 0.063 %), and Stock *et al.*[50] (AAD = 0.10 %) were

reproduced within 0.3 %. The data of Giauque and Wiebe[24] (AAD = 0.48 %) exhibit a systematic positive offset, which may be caused by an impurity of phosphorus pentoxide that they observed in their sample.

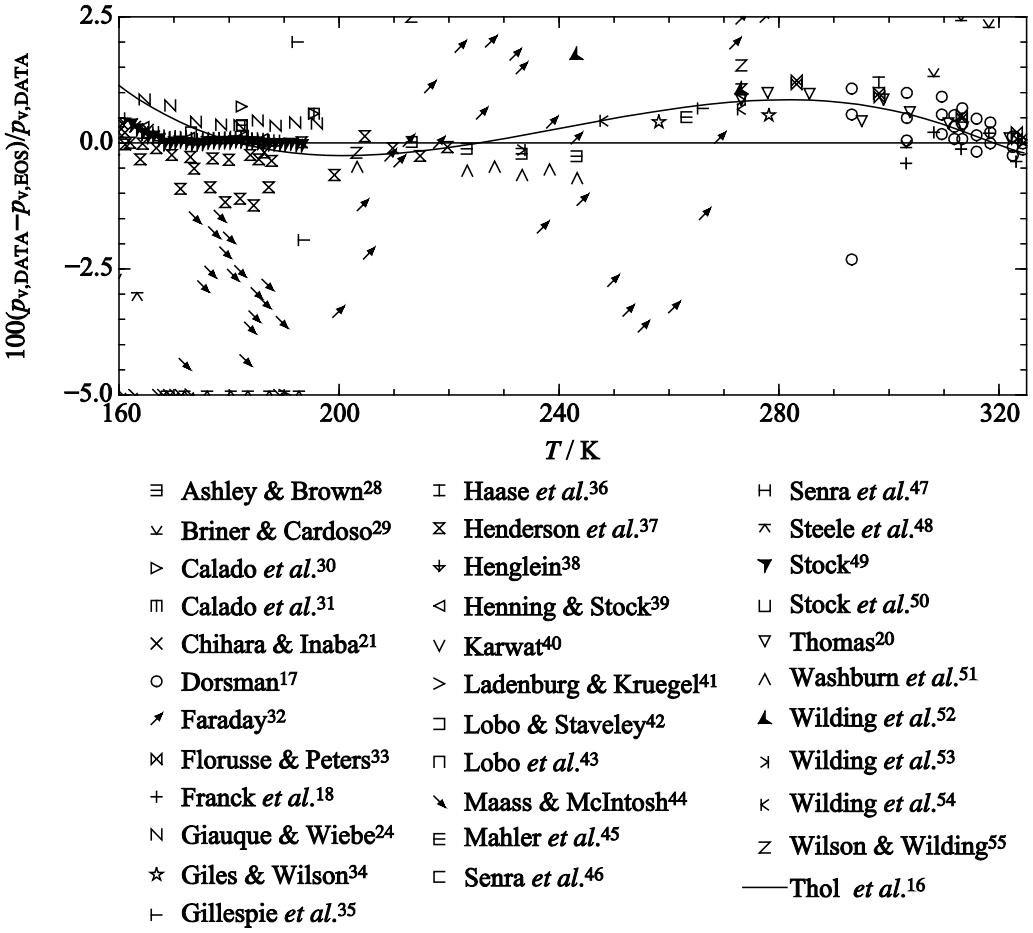

Figure 10. Percentage deviations of experimental vapor pressure data from the present equation of state. The equation of Thol *et al.*[16] is shown for comparison.

The data of Maass and McIntosh[44] exhibit a scatter of more than 5 %, which is in agreement with their measurements on hydrogen sulfide carried out with the same apparatus. The vapor pressure data of Steele *et al.*[48] systematically deviate by approximately −11 % from the present equation of state. The high temperature region ($T > 280$ K) was mainly investigated by Dorsman,[17] Florusse and Peters,[33] Franck *et al.*,[18] and Thomas.[20] Their results agree with each other within 0.6 %. The most recent data of Florusse and Peters[33] were investigated with a sample purity of 99.5 % in a high pressure Caille apparatus. At each temperature, two measurements were carried out, which deviate only by 0.1 % from each other. The specified uncertainties of $\Delta T = 0.02$ K and $\Delta p = 0.002$ MPa lead to a combined expanded uncertainty ($k = 2$) of 0.1 % to 0.5 %. However, during their experiment, they observed the formation of white precipitates in the presence of oxygen. This fact also has to be considered in the uncertainty analysis because sample purity may have a strong impact. Deviations with respect to the present equation of state decrease from 1.2 % at 283 K to < 0.1 % near the critical point.

Due to the impurity of the sample, this deviation is still assumed to be adequate (AAD = 0.58 %). The data of Dorsman[17] (AAD = 0.43 %) scatter around the present equation within 1 %. Unfortunately, his dissertation from 1908 is not available so that the quality of the data cannot be determined. Measurements of the vapor pressure by Thomas[20] are represented within 1 % (AAD = 0.61 %). He reports a 1 % uncertainty of the total pressure. However, the sample purity of 99.7 %, as stated by the manufacturer, was not confirmed and not considered in the uncertainty analysis. His own correlation can only reproduce the underlying dataset within 0.3 %. The data of Franck *et al.*[18] were determined with a questionable approach, as discussed in section 4.1. Therefore, these data were not considered in the present fitting procedure, although they are reproduced within 0.4 % (AAD = 0.26 %). In the medium temperature range, no clear decision could be made of which data are correct. Extrapolating from the low temperature region, the course of the data of Ashley and Brown[28] matches with the data of Henderson *et al.*,[37] which are reproduced within 0.26 % (AAD = 0.61 %). Despite a constant offset of approximately –0.55 %, the data of Washburn *et al.*[51] confirm this trend. Extending the high temperature data into the medium temperature range, some recent data of Giles and Wilson[34] and Wilding *et al.*[53,54] exhibit a positive offset with respect to the present equation and the low temperature data. Therefore, none of the data in the medium temperature range were used for the development of the present equation of state. For a reliable assessment, new measurements are required. Based on these findings, the uncertainty of the present equation of state in terms of the vapor pressure is expected to be 0.5 % for $T < 250$ K and 1 % for higher temperatures.

The saturated liquid and vapor densities were less comprehensively investigated by experiment than the vapor pressure. For the saturated liquid density, only eight datasets are available in the literature, cf. Table 6. Similar to the properties discussed above, most of them were published more than 50 years ago. The lower temperature range ($T < 200$ K) was investigated by Henderson *et al.*,[37] Steele *et al.*,[48] and Kanda.[56] Two different trends can be observed here. The data of Steele *et al.*[48] and Kanda[56] agree with each other, but exhibit a negative slope in the corresponding deviation plot, cf. Figure 11 (top). The present equation of state follows the data of Henderson *et al.*[37] These data were determined about 50 to 80 years later than the other ones, but they were not adopted as the most accurate data by default. Especially the mutual agreement of Steele *et al.*[48] and Kanda[56] could be an indication that these values might be preferable. Therefore, only homogeneous densities were used in the fitting process. This approach showed that the saturated liquid density data of Henderson *et al.*[37] match with the homogeneous density data. They were chosen to be fitted in the lower temperature range. The apparatus employed by Henderson *et al.*[37] was also used by Terry *et al.*[65] to measure the saturated liquid density of several gases, such as methane and oxygen. Henderson *et al.*[37] found a systematic offset of +0.2 % when comparing the data of Terry *et al.*[65] with other literature values. With respect to the most recent reference equations of state[61,66] for those fluids,

the offset is even higher. Therefore, Henderson *et al.*[37] corrected their measurements by 0.2 %, but do not state an experimental uncertainty. Except for a single data point at 236.5 K, all data can be reproduced with the present equation of state within 0.2 % (AAD = 0.094 %).

The high temperature region was studied by Dorsman,[17] Rupert,[57] and Thomas.[20] All of them agree with each other within approximately 0.8 %. Since the data of Dorsman[17] and Rupert[57] are more than 100 years old, it is difficult to assess the accuracy of their measurements. Except for a single data point at 309.3 K, the most recent saturated liquid density measurements of Thomas[20] agree within 0.25 % with the present equation of state (AAD = 0.15 %). Based on the limited information, the uncertainty of the present equation of state with respect to the saturated liquid density is expected to be 0.5 % for $T < 240$ K and 1 % for higher temperatures.

For the saturated vapor density, no reliable measurements are available (cf. Figure 11, bottom). Therefore, no accuracy specification for the present equation of state can be made for this property.

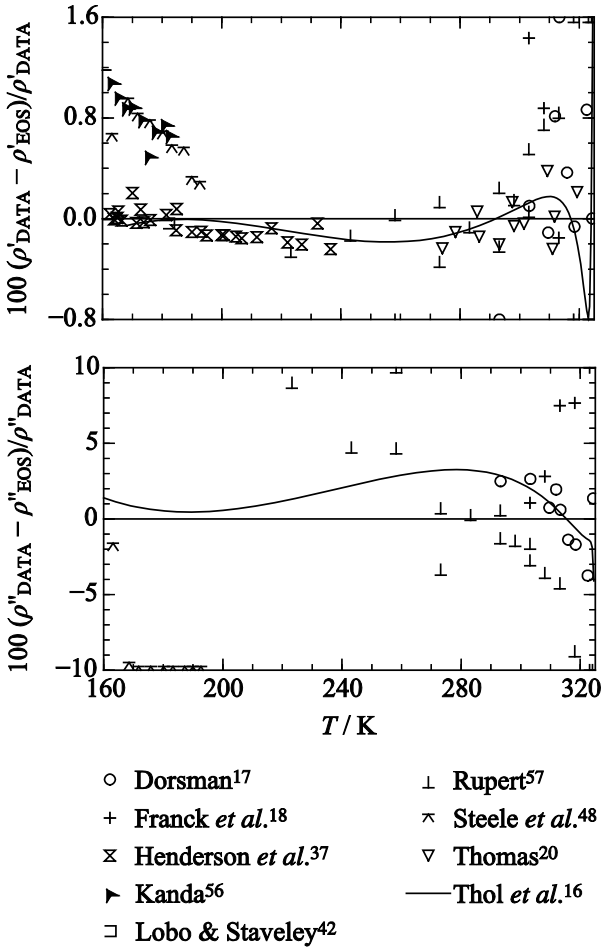

Figure 11. Percentage deviations of experimental saturated liquid and vapor density data from the present equation of state. The equation of Thol *et al.*[16] is shown for comparison.

The calculation of vapor-liquid equilibrium data requires iterative and time-consuming calculations. Therefore, ancillary equations for vapor pressure, saturated liquid density, and saturated vapor density were developed:

$$\ln\left(\frac{p_\mathrm{v}}{p_\mathrm{c}}\right)=\left(\frac{T_\mathrm{c}}{T}\right)\sum_{i=1}^{5}n_i\left(1-\frac{T}{T_\mathrm{c}}\right)^{t_i}, \tag{10}$$

$$\frac{\rho'}{\rho_\mathrm{c}}=1+\sum_{i=1}^{5}n_i\left(1-\frac{T}{T_\mathrm{c}}\right)^{t_i}, \tag{11}$$

and

$$\ln\left(\frac{\rho''}{\rho_\mathrm{c}}\right)=\sum_{i=1}^{6}n_i\left(1-\frac{T}{T_\mathrm{c}}\right)^{t_i}. \tag{12}$$

Using initial values from these correlations significantly reduces computation time of software tools such as TREND,[67] REFPROP,[68] and CoolProp.[69] The corresponding parameters are listed in Table 7 and deviations with respect to the present equation of state are illustrated in Figure 12.

Table 7. Parameters of the ancillary equations for vapor pressure, saturated liquid density, and saturated vapor density.

	Vapor pressure, Eq. (10)		**Saturated liquid density, Eq. (11)**		**Saturated vapor density, Eq. (12)**	
i	n_i	t_i	n_i	t_i	n_i	t_i
1	−6.73	1.00	2.547	0.418	−2.5676	0.417
2	1.464	1.50	−0.631	1.12	−4.1055	0.923
3	−1.994	3.12	1.75	1.86	−12.068	2.57
4	1.283	3.95	−1.922	2.66	−29.03	5.54
5	−2.062	4.8	1.03	3.57	−54.93	10.5
6					−222.7	23.3

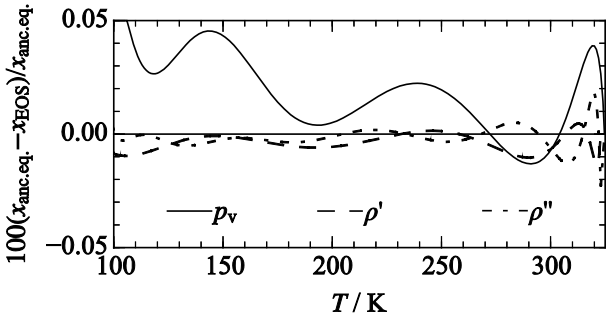

Figure 12. Percentage deviation of the ancillary equations for the vapor pressure and the saturation densities from the present equation of state.

4.3 Representation of the Critical Point

One of the main issues of the equation of Thol *et al.*[16] is its incorrect behavior around the critical point. Therefore, special attention was paid in this work to the correct representation of that region. Table 8 lists the critical parameters available in the literature.

Table 8. Critical parameters of hydrogen chloride from the literature.

Author	Year	T_c / K	ρ_c / (mol·dm^{-3})	p_c / MPa
Briner [70]	1906	324.93	-	8.471
Cardoso & Germann [71]	1912	324.53	-	8.263
Florusse & Peters [33]	2002	324.60	-	8.309
Franck *et al.* [18]	1962	324.63	12.34	8.258
Grosh *et al.* [25]	1965	324.53	11.27	8.263
Kooper [72]	1936	324.13	-	-
Leduc [73]	1909	325.18	-	8.410
Leduc & Sacerdote [74]	1897	325.13	-	8.410
Thomas [20]	1962	324.67	-	8.306
Vincent & Chappuis [75]	1885	324.38	-	-
Vincent & Chappuis [76]	1885	324.63	-	9.727

Most of the critical temperature data scatter around 324.6 K. Thol *et al.*[16] selected the value of Grosh *et al.*[25] because they also provide a critical density. For the present equation of state, the temperature of Thomas was taken as a starting point. During the fitting procedure, it was found that a slightly higher value enables a better representation of density and speed of sound data. The critical density was also determined by the fitting procedure. The final value of 11.87 mol·dm^{-3} is located between the two values from the literature. In contrast to Thol *et al.*,[16] a non-linear fitting technique, which is nowadays applied for the development of modern equations of state, was used in this work. In this way, not only experimental data, but also constraints could be applied to the fit. Thereby, the rectilinear diameter $\rho_{RD} = (\rho' + \rho'')/2$ was specified to be a straight line approaching the critical point, following Zollweg and Mulholland.[77] Furthermore, a saddle point of the critical isotherm was ensured at the critical point by forcing the first and second pressure derivatives with respect to the density to vanish

$$\left(\frac{\partial p}{\partial \rho}\right)_{T_c} = 0 \quad \text{and} \quad \left(\frac{\partial^2 p}{\partial \rho^2}\right)_{T_c} = 0 . \tag{13}$$

Figure 13 shows that both requirements are fulfilled by the present equation of state. In contrast, the critical isotherm of the equation of Thol *et al.*[16] exhibits no saddle point, but an inflection point, so that it is technically subcritical.

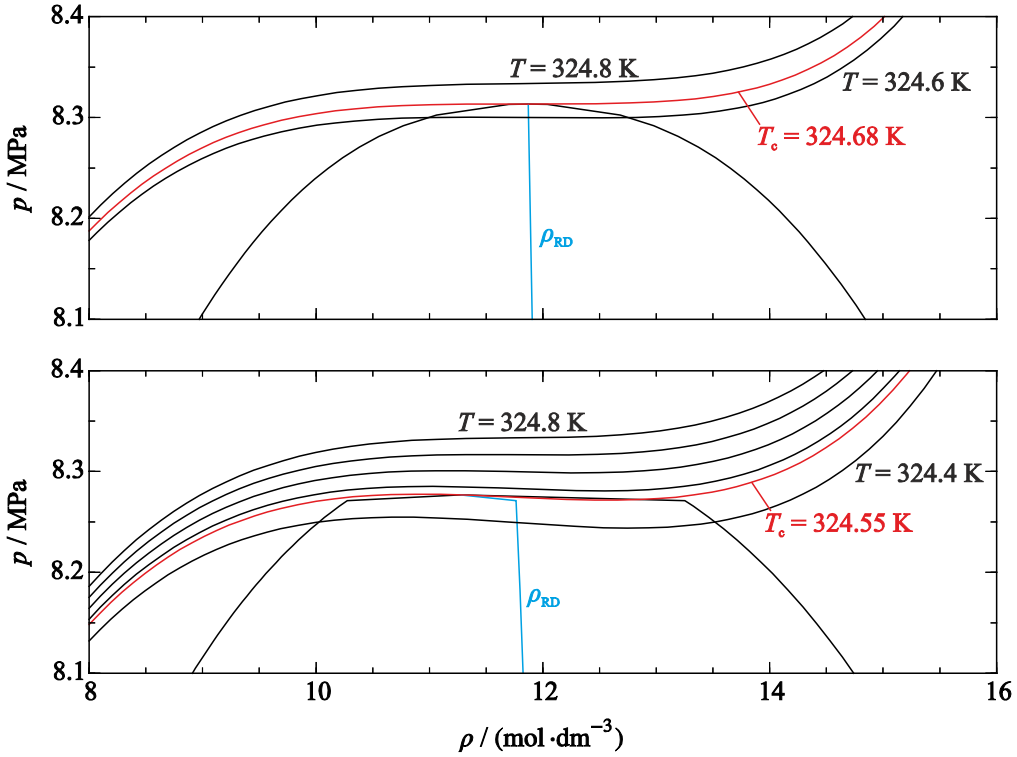

Figure 13. p,ρ-diagrams calculated with the present equation of state (top) and the equation of Thol *et al.*[16] (bottom) including the critical isotherm (red curve) and the rectilinear diameter (ρ_{RD}).

The resulting critical pressure of the present equation of state p_c = 8.3135 MPa was calculated from the final expression. It is in good agreement with the values reported in the literature, cf. Table 8.

4.4 Caloric Properties

The speed of sound measurements carried out in this work led to the only data available for this property. The measurement procedure as well as the experimental uncertainties are comprehensively discussed in section 2. Figure 14 shows that the data are mostly reproduced within the experimental uncertainty of the employed apparatus.

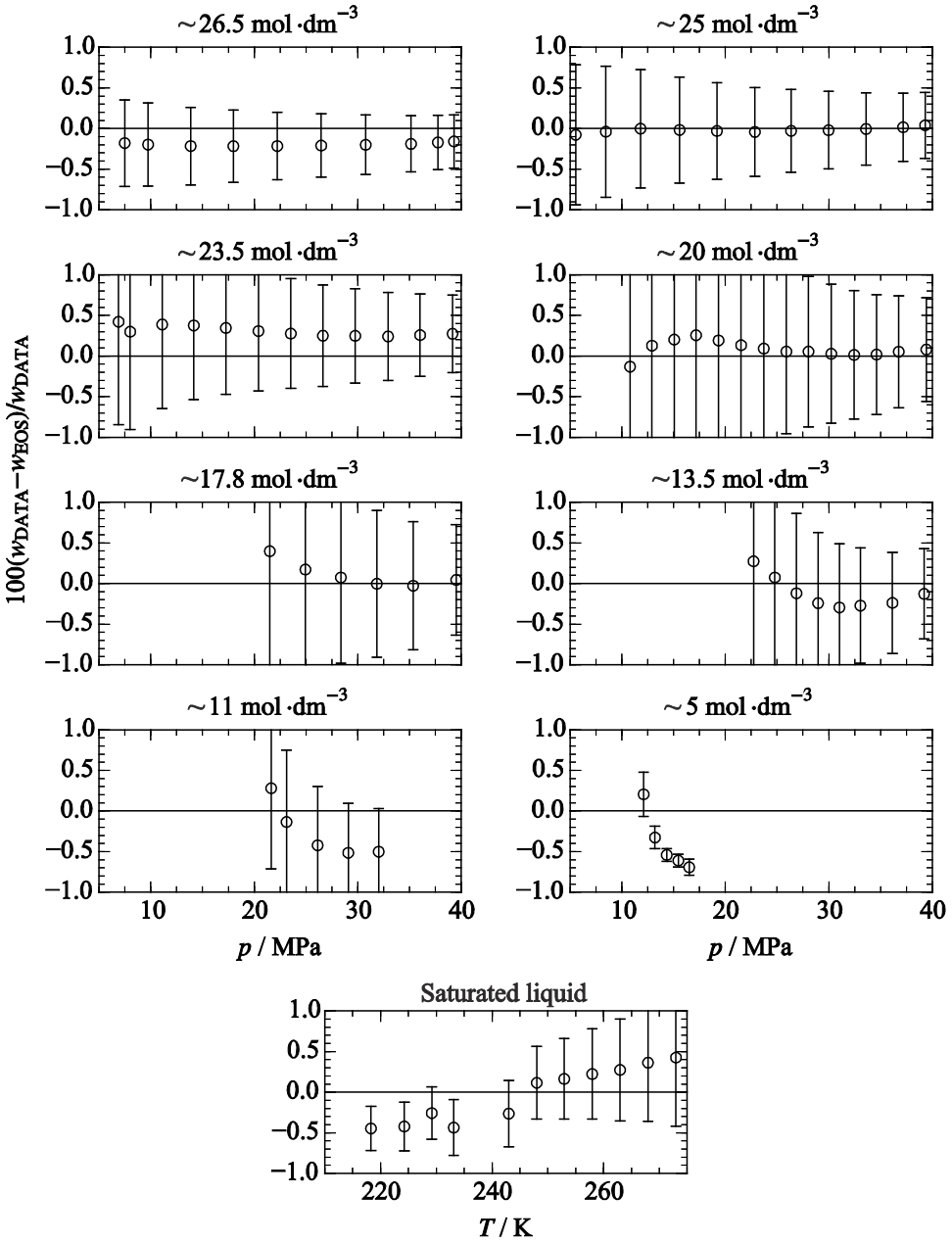

Figure 14. Percentage deviation of the speed of sound measurements carried out in this work from the present equation of state.

Except for the two lowest quasi-isochors, deviations are generally within 0.3 %. The overall uncertainty including the sample purity could not be determined because of missing sample analysis. Therefore, even the deviations at the lower isochors and the low temperatures along the saturated liquid line are assumed to be reasonable. A more accurate description was not possible without compromizing the homogeneous density data. However, as described in section 4.1, the available density data are rather old and have considerable experimental uncertainties. Thus, new density measurements would be highly valuable to validate the data assessment.

In addition to the present experimental data, some heat capacity measurements are available. The isochoric heat capacity was measured by Franck *et al.*[18] with the same

apparatuses as the density. They deviate by more than 10 % from the present equation of state (AAD = 7.1 %) for low temperatures. This is not surprising when considering the issues during their measurements discussed in section 4.1. Therefore, a reasonable statement about the uncertainty of the present equation of state cannot be made. In Figure 15, relative deviations of isobaric heat capacity data in the saturated liquid state from the present equation of state are depicted in a rather limited temperature range (158 K to 190 K). Three different trends can be observed. The data of Eucken and Karwat[23] (AAD = 4.1 %) exhibit a systematic deviation of approximately 4 %. The datasets of Chiara and Inaba[21] (AAD = 4.2 %), Giauque and Wiebe[24] (AAD = 3.4 %), and Grosh *et al.*[25] (AAD = 3.8 %) agree with each other within 0.5 %, but deviate by 2.5 % to 5 % from the present equation of state. Finally, the data of Clusius[22] (AAD = 0.28 %) scatter within 1 % around the equation. The equation of Thol *et al.*[16] matches the data of Chiara and Inaba,[21] Giauque and Wiebe,[24] and Grosh *et al.*[25] because it was adjusted to them. For the present equation of state, an attempt was made to adjust the most recent data more accurately, but this led to a systematic shift of the speed of sound data along the saturated liquid line. Thus, none of these data were used during the fitting procedure.

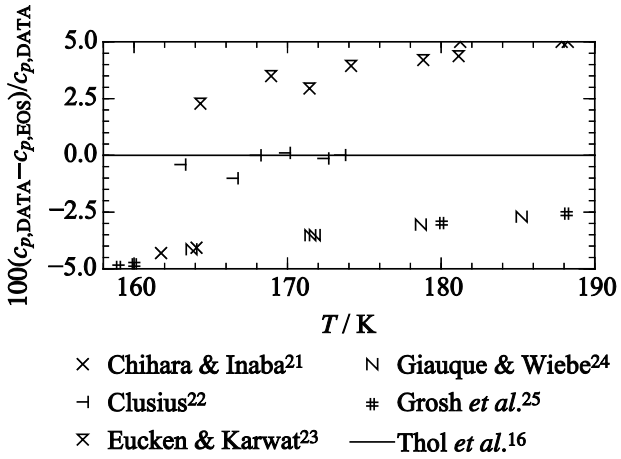

Figure 15. Percentage deviation of experimental isobaric heat capacity data from the present equation of state.

5 Conclusion

Speed of sound measurements for hydrogen chloride in the liquid and dense vapor phases were presented. Because they are the first data for this property in the literature, they are important for modeling caloric data. Based on these measurements and other data types from the literature, a fundamental equation of state for hydrogen chloride was developed. It is formulated in terms of the Helmholtz energy and can be used to calculate all thermodynamic properties by combinations of the function itself and derivatives with respect to its natural variables. Based on the available experimental data, it is valid from the triple point temperature 159.07 K to 480 K and up to a maximum pressure of 40 MPa. Assuming that the data of Franck *et al*.[18] are reasonable, this range may be extended to 670 K and 200 MPa. The accuracy of the equation was analyzed by extensive comparisons to experimental data. Furthermore, the physical and extrapolation behavior of the equation of state was carefully monitored, which is an important aspect for the application to mixture models.

In the supplementary material, a fluid file for the application in the software packages TREND[67] and REFPROP[68] is provided.

Acknowledgement

The authors thank R. Kuska and Dr. E. W. Lemmon for their support during the development of the equation of state.

Supporting Information Available

A text file containing the parameters of the equation is available. For the use in TREND[67] or REFPROP[68], it has to be renamed into HCl.FLD.

6 References

(1) Air Liquid. *Sicherheitsdatenblatt gemäß RL 1907/2006/EG (REACH)*, **Versions-Nr.: 2-01**.

(2) Air Liquid, Chlorwasserstoff N28. *Air Liquide's Gas Encyclopedia*, **2009**; pp 771–778.

(3) Dubberke, F. H.; Baumhögger, E.; Vrabec, J., Burst Design and Signal Processing for the Speed of Sound Measurement of Fluids with the Pulse-echo Technique. *Rev. Sci. Instrum.* **2015**, *86*, 054903.

(4) Austin, J. B., The Heat Capacity of Some Hydrogen Halides at High Temperatures as Calculated from Raman Spectra. *J. Am. Chem. Soc.* **1932**, *54*, 3459–3460.

(5) Salant, E. O.; Sandow, A., Raman Scattering from HCl Liquid. *Science* **1929**, *69*, 357.

(6) Potter, R. L., Thermodynamic Functions of Some Chlorine Compounds. *J. Chem. Phys.* **1959**, *31*, 1100–1103.

(7) Herzberg, G. *Molecular Spectra and Molecular Structure: I. Spectra of Diatomic Molecules*, 2nd edition 1; Van Nostrand: New York, **1950**.

(8) Gilbert, D. A.; Roberts, A.; Griswold, P. A., Nuclear and Molecular Information from the Microwave Spectrum of FCl. *Phys. Rev.* **1949**, *76*, 1723.

(9) Hurly, J. J., Thermophysical Properties of Chlorine from Speed-of-Sound Measurements. *Int. J. Thermophys.* **2002**, *23*, 455–475.

(10) Lemmon, Eric W. *Numerical Fitting Algorithm for the Development of Equations of State*, personal communication, **2016**.

(11) Lemmon, E. W.; Jacobsen, R. T., A New Functional Form and New Fitting Techniques for Equations of State with Application to Pentafluoroethane (HFC-125). *J. Phys. Chem. Ref. Data* **2005**, *34*, 69–108.

(12) Lemmon, E. W.; McLinden, M. O.; Wagner, W., Thermodynamic Properties of Propane. III. A Reference Equation of State for Temperatures from the Melting Line to 650 K and Pressures up to 1000 MPa. *J. Chem. Eng. Data* **2009**, *54*, 3141–3180.

(13) Thol, M.; Lemmon, E. W., Equation of State for the Thermodynamic Properties of trans-1,3,3,3-Tetrafluoropropene [R1234ze(E)]. *Int. J. Thermophys.* **2016**, *37*, 28.

(14) Gao, K.; Wu, J.; Zhang, P.; Lemmon, E. W., A Helmholtz Energy Equation of State for Sulfur Dioxide. *J. Chem. Eng. Data* **2016**, *61*, 2859–2872.

(15) Thol, M.; Rutkai, G.; Köster, A.; Span, R.; Vrabec, J.; Lustig, R., Equation of State for the Lennard-Jones Fluid. *J. Phys. Chem. Ref. Data* **2016**, *45*, 023101.

(16) Thol, M.; Piazza, L.; Span, R., A New Functional Form for Equations of State for Some Weakly Associating Fluids. *Int. J. Thermophys.* **2014**, *35*, 783–811.

(17) Dorsman, C., Hydrogen Chloride. Ph.D. thesis, Universiteit van Amsterdam, Amsterdam, **1908**.

(18) Franck, E. U.; Brose, M.; Mangold, K., Supercritical Hydrogen Chloride. Specific Heat up to 300C and 300atm. PVT-Data up to 400C and 2000atm. *Prog. Int. Res. Thermodyn. Transp. Prop., Symp. Thermophys. Prop., 2nd* **1962**, 159–165.
(19) Nunes Da Ponte, M.; Staveley, L. A. K., The Equation of State and Thermodynamic Properties of Liquid Hydrogen Chloride. *J. Chem. Thermodyn.* **1981**, *13*, 179–186.
(20) Thomas, W., Volumetric Behavior of Hydrogen Chloride. *Prog. Int. Res. Thermodyn. Transp. Prop., Symp. Thermophys. Prop., 2nd* **1962**, 166–171.
(21) Chihara, H.; Inaba, A., Thermodynamic Properties of Solid Hydrogen Halides and Deuterium Halides: I. HCl and DCl. *J. Chem. Thermodyn.* **1976**, *8*, 915–934.
(22) Clusius, K., Über die spezifische Wärme einiger kondensierter Gase zwischen 10° abs. und ihrem Tripelpunkt. *Z. Phys. Chem.* **1929**, *3B*, 41–79.
(23) Eucken, A.; Karwat, E., Die Bestimmung des Wärmeinhaltes einiger kondensierter Gase. *Z. Phys. Chem. Stoechiom. Verwandschafts.* **1924**, *112*, 467–485.
(24) Giauque, W. F.; Wiebe, R., The Entropy of Hydrogen Chloride. Heat Cpacity from 16°K. to boiling Point. Heat of Vaporization. Vapor Pressures of Solid and Liquid. *J. Am. Chem. Soc.* **1928**, *50*, 101–122.
(25) Grosh, J.; Jhon, M. S.; Ree, T.; Eyring, H., The Significant Structure Theory Applied to Liquid Hydrogen Halides. *Proc. Natl. Acad. Sci. U. S. A.* **1965**, *54*, 1004–1009.
(26) Schramm, B.; Leuchs, U., Zweite Virialkoeffizienten von HCl, DCl und Ar - HCl-Mischungen. *Ber. Bunsen Ges. Phys. Chem.* **1979**, *83*, 847–852.
(27) Wormald, C. J.; Massucci, M., The Excess Enthalpy of {yAr + (1−y)HCl} (g) and the Second Virial Coefficient of HCl from T = 210 K to T = 370 K. *J. Chem. Thermodyn.* **1997**, *29*, 3–14.
(28) Ashley, J. H.; Brown, G. M., Vapor-Liquid Equilibria - Hydrogen Chloride-Ethane. *Chem. Eng. Prog. Symp. Ser.* **1954**, *50*, 129–136.
(29) Briner, E.; Cardoso, E., Recherches sur la Liquéfaction et la Compressibilité des Mélanges Gazeux. *J. Chim. Phys. Phys.-Chim. Biol.* **1908**, *6*, 641–680.
(30) Calado, J. C. G.; Kozdon, A. F.; Morris, P. J.; Nunes Da Ponte, M.; Staveley, L. A. K.; Woolf, L. A., Thermodynamics of Liquid Mixtures of Xenon and Hydrogen Chloride. *J. Chem. Soc. Faraday Trans. 1* **1975**, *71*, 1372–1375.
(31) Calado, J. C. G.; Gray, C. G.; Gubbins, K. E.; Palavra, António M. F.; Soares, Virgílio A. M.; Staveley, L. A. K.; Twu, C.-H., Thermodynamics of Binary Liquid Mixtures Involving Hydrogen Bromide, Hydrogen Chloride and Xenon. *J. Chem. Soc. Faraday Trans. 1* **1978**, *74*, 893–911.
(32) Faraday, M., On the Liquefaction and Solidification of Bodies Generally Existing as Gases. *Phil. Trans. Roy. Soc. London* **1845**, *135*, 155–177.
(33) Florusse, L.; Peters, C. J., Vapor-Liquid Phase Behavior of Binary Systems of Hydrogen Chloride and Certain n-Alkanes. *Fluid Phase Equilib.* **2002**, *202*, 1–11.

(34) Giles, N. F.; Wilson, G. M., Phase Equilibria on Seven Binary Mixtures. *J. Chem. Eng. Data* **2000**, *45*, 146–153.
(35) Gillespie, P. C.; Cunningham, J. R.; Wilson, G. M., Total Pressure and Infinite Dilution Liquid Equilibrium Measurements for the Ethylene Oxide/Water System. *AlChE Symp. Ser.* **1985**, *244*, 26–40.
(36) Haase, R.; Naas, H.; Thumm, H., Experimentelle Untersuchungen über das thermodynamische Verhalten konzentrierter Halogenwasserstoffsäuren. *Z. Phys. Chem.* **1963**, *37*, 210–229.
(37) Henderson, C.; Lewis, D.; Prichard, P.; Staveley, L. A. K.; Fonseca, I. M. A.; Lobo, L. Q., Some Thermodynamic Properties of Hydrogen Chloride and Deuterium Chloride. *J. Chem. Thermodyn.* **1986**, *18*, 1077–1088.
(38) Henglein, F. A., Dampfdrucke und Kristallgitter der Halogenwasserstoffe. *Z. Physik* **1923**, *18*, 64–69.
(39) Henning, F.; Stock, A., Über die Sättigungsdrucke einiger Dämpfe zwischen +10 und −181°. *Z. Physik* **1921**, *4*, 226–240.
(40) Karwat, E., Der Dampfdruck des festen Chlorwasserstoffs, Methans und Ammoniaks. *Z. Phys. Chem. Stoechiom. Verwandschafts.* **1926**, *112*, 486–490.
(41) Ladenburg, A.; Kruegel, C., Ueber die Messung tiefer Temperaturen. II. *Ber. Dtsch. Chem. Ges.* **1900**, *33*, 637–646.
(42) Lobo, L. Q.; Staveley, L. A. K., Thermodynamics of Liquid (Hydrogen Chloride + Dinitrogen Oxide). *J. Chem. Thermodyn.* **1984**, *16*, 653–659.
(43) Lobo, L. Q.; Staveley, L. A. K.; Venkatasubramanian, V.; Clancy, P.; Gubbins, K. E.; Gray, C. G.; Joslin, C. G., Thermodynamic Properties of Liquid Mixtures of Hydrogen Chloride and Tetrafluoromethane. *Fluid Phase Equilib.* **1985**, *22*, 89–105.
(44) Maass, O.; McIntosh, D., The Vapour Pressures of the Halogen Hydrides and of Hydrogen Sulphide. *Trans. R. Soc. Can.* **1914**, *8*, 65–71.
(45) Mahler, B. A.; Felix, V. M.; Miller, R. N., Azeotrope und azeotropartige Zusammensetzungen und Verfahren zur Trennung von HCl und Halogenkohlenwasserstoffen Patent No. Patent DE 694 17 024 T 2.
(46) Senra, A. M. P.; Fonseca, I. M. A.; Ferreira, A. G. M.; Lobo, L. Q., Vapour-Liquid Equilibria of {xCH3F+(1−x)HCl} at Temperatures of 159.01 K and 182.33 K. *J. Chem. Thermodyn.* **2002**, *34*, 1557–1566.
(47) Senra, A. M. P.; Fonseca, I. M. A.; Lobo, L. Q., (Vapour+Liquid) Equilibria of {xCH3Cl+(1−x)HCl} at Temperatures (159.01 and 182.33) K. *J. Chem. Thermodyn.* **2005**, *37*, 627–630.
(48) Steele, B. D.; McIntosh, D.; Archibald, E. H., Die Halogenwasserstoffsäuren als leitende Lösungsmittel. *Z. Phys. Chem.* **1906**, *55*, 129–199.

(49) Stock, A., Dampfdruck-Thermometer. *Z. Elektrochem. Angew. Phys. Chem.* **1923**, *29*, 354–358.
(50) Stock, A.; Henning, F.; Kuß, E., Dampfdruckdaten für Temperaturbestimmungen zwischen +25° und -185°. *Ber. Dtsch. Chem. Ges.* **1921**, *54*, 1119–1129.
(51) Washburn, E. W.; West, C. J.; Hull, C. *International Critical Tables of Numerical Data, Physics, Chemistry, and Technology: Volume III.*; McGraw-Hill: New York, **1926**.
(52) Wilding, W. V.; Wilson, L. C.; Wilson, G. M., Vapor-Liquid Equilibrium Measurements on Five Binary Mixtures. *Fluid Phase Equilib.* **1987**, *36*, 67–90.
(53) Wilding, W. V.; Giles, N. F.; Wilson, L. C., Phase Equilibrium Measurements on Nine Binary Mixtures. *J. Chem. Eng. Data* **1996**, *41*, 1239–1251.
(54) Wilding, W. V.; Adams, K. L.; Carmichael, A. E.; Hull, J. B.; Jarman, T. C.; Jenkins, K. P.; Marshall, T. L.; Wilson, H. L., Vapor-Liquid Equilibrium Measurements on Three Binary Mixtures: Difluoromethane/Hydrogen Chloride, cis -1,3-Dichloropropene/ trans -1,3-Dichloropropene, and Pyrrole/Water. *J. Chem. Eng. Data* **2002**, *47*, 748–756.
(55) Wilson, H. L.; Wilding, W. V., Experimental Results for DIPPR 1990-91 Projects on Phase Equilibria and Pure Component Properties, Vapor-Liquid and Liquid-Liquid Equilibrium Measurements on Twenty-Two Binary Mixtures. *DIPPR Data Series* **1994**, *2*, 63–115.
(56) Kanda, E., Studies on Fluorine at Low Temperatures: VII. Determination of Dielectric Constants of Condensed Gases. *Bull. Chem. Soc. Jpn.* **1937**, *12*, 473–479.
(57) Rupert, F. F., A Study of the System Hydrogen Chloride and Water. *J. Am. Chem. Soc.* **1909**, *31*, 851–866.
(58) Wieser, M. E.; Berglund, M., Atomic Weights of the Elements 2007 (IUPAC Technical Report). *Pure Appl. Chem.* **2009**, *81*, 2131–2156.
(59) Nunes Da Ponte, M.; Streett, W. B.; Staveley, L. A. K., An Experimental Study of the Equation of State of Liquid Mixtures of Nitrogen and Methane, and the Effect of Pressure on their Excess Thermodynamic Functions. *J. Chem. Thermodyn.* **1978**, *10*, 151–168.
(60) Span, R.; Lemmon, E. W.; Jacobsen, R. T.; Wagner, W.; Yokozeki, A., A Reference Equation of State for the Thermodynamic Properties of Nitrogen for Temperatures from 63.151 to 1000 K and Pressures to 2200 MPa. *J. Phys. Chem. Ref. Data* **2000**, *29*, 1361–1433.
(61) Setzmann, U.; Wagner, W., A New Equation of State and Tables of Thermodynamic Properties for Methane Covering the Range from the Melting Line to 625 K at Pressures up to 100 MPa. *J. Phys. Chem. Ref. Data* **1991**, *20*, 1061–1155.
(62) Kihara, T., Virial Coefficients and Models of Molecules in Gases. *Rev. Mod. Phys.* **1953**, *25*, 831–843.
(63) Span, R.; Wagner, W., On the Extrapolation Behavior of Empirical Equations of State. *Int. J. Thermophys.* **1997**, *18*, 1415–1443.

(64) Lobo, L. Q.; Staveley, L. A. K.; Clancy, P.; Gubbins, K. E., Enthalpy of Mixing of Liquid Hydrogen Chloride and Liquid Xenon. Comparison of Experiment and Theory. *J. Chem. Soc. Faraday Trans. 1* **1980**, *76*, 174–179.
(65) Terry, M. J.; Lynch, J. T.; Bunclark, M.; Mansell, K. R.; Staveley, L. A. K., The Density of Liquid Argon, Krypton, Xenon, Oxygen, Nitrogen, Carbon Monoxide, Methane, and Carbon Tetrafluoride Along the Orthobaric Liquid Curve. *J. Chem. Thermodyn.* **1969**, *1*, 413–424.
(66) Schmidt, R.; Wagner, W., A New Form of the Equation of State for Pure Substances and Its Application to Oxygen. *Fluid Phase Equilib.* **1985**, *19*, 175–200.
(67) Span, R.; Eckermann, T.; Herrig, S.; Hielscher, S.; Jäger, A.; Thol, M. *TREND. Thermodynamic Reference and Engineering Data 3.0*; Lehrstuhl für Thermodynamik, Ruhr-Universität Bochum: Bochum, Germany, **2016**.
(68) Lemmon, E. W.; Bell, I. H.; Huber, M. L.; McLinden, M. O. *NIST Standard Reference Database 23: Reference Fluid Thermodynamic and Transport Properties-REFPROP, Version 9.1.1*; National Institute of Standards and Technology: Gaithersburg, USA, **2014**.
(69) Bell, I. H.; Wronski, J.; Quoilin, S.; Lemort, V., Pure and Pseudo-pure Fluid Thermophysical Property Evaluation and the Open-Source Thermophysical Property Library CoolProp. *Ind. Eng. Chem. Res.* **2014**, *53*, 2498–2508.
(70) Briner, E., Compressibilité de Mélanges de Gaz Susceptibles de Réagir entre eux pour former des Composés Solides ou Liquides. Tensions de Vapeur et Constantes Critiques des Gaz: Acide Chlorhydrique, Hydrogène, Phosphoré et Acide Sulfureux. *J. Chem. Phys.* **1906**, *4*, 476–485.
(71) Cardoso, E.; Germann, A.-F.-O., Constantes Critiques de L'Acide Chlorhydrique. *J. Chim. Phys. Phys.-Chim. Biol.* **1912**, *10*, 517–519.
(72) Kooper, H., Kritische Temperaturen einiger einfacher Deuteriumverbindungen. *Z. Phys. Chem. (Leipzig)* **1936**, *175*, 469–472.
(73) Leduc, A., Compressibilité des Gaz entre 0 atm et à toute Temperature. *C.R. Hebd. Seances Acad. Sci.* **1909**, *148*, 407–410.
(74) Leduc, A.; Sacerdote, P., Constantes Critiques de quelques Gaz. *C.R. Hebd. Seances Acad. Sci.* **1897**, *125*, 397–398.
(75) Vincent, C.; Chappuis, J., Sur les Tensions et les Points Critique de quelques Vapeurs. *C.R. Hebd. Seances Acad. Sci.* **1885**, *100*, 1216–1218.
(76) Vincent, C.; Chappuis, J., Sur les Températures et les Pressions Critiques de quelques Vapeurs. *C.R. Hebd. Seances Acad. Sci.* **1885**, *101*, 427–429.
(77) Zollweg, J. A.; Mulholland, G. W., On the Law of the Rectilinear Diameter. *J. Chem. Phys.* **1972**, *57*, 1021–1025.